RAIN RATE PROFILING WITH AN ATTENUATING RADAR OVER THE OCEAN

Masaharu Fujita
Communications Research Laboratory
Koganei, Tokyo 184, Japan

INTRODUCTION

Global activity of rain plays an important role for world climate condition as well as water budget. To have a more quantitative knowledge about the rain activity, rain mapping satellite projects are now being proposed such as TRMM (Simpson et al., 1988) and BEST (Marzoug et al., 1988). The most important sensor for the satellites is a radar by which rain rate distribution would be measured quantitatively in vertical and horizontal directions. As a satellite radar, there are some limitations in size, power consumption and others. To increase an EIRP (effective isotropic radiation power) within the limitation, it would be natural to choose a high radar frequency above 10 GHz; however, the other problem arises of radar wave attenuation due to rain itself.

In this article, the author will propose a new estimation technique of rain rate profiles with a rain-attenuating radar over the ocean.

ALGORITHM

A radar equation for an attenuating frequency is given as follows:

$$P = \frac{CZF}{r^2} 10^{-0.2\int_0^r k dr}, \qquad (1)$$

where P : average received power,
C : radar constant including a dielectric factor of raindrops,
Z : radar reflectivity,
F : radar calibration factor,
r : range,
k : attenuation coefficient of radar wave.

The radar calibration factor consists of two parts, i.e., internal and external terms. We would be able to determine an internal term with an appropriately designed hardwares. An external calibration factor is usually determined by observing a target having a known radar cross section. For a satellite radar, however, it would be difficult to perform an external calibration for rain through observation. Here, we remove the term F by evaluating a relative value of received powers at adjacent range bins. Rewriting (1) on range bin basis and changing it in log scale, the ratio is expressed as follows:

$$\log P(i+1) - \log P(i) + 2\{\log r(i+1) - \log r(i)\} = \log Z(i+1) - \log Z(i) - 0.1d\{k(i)+k(i+1)\}, \qquad (2)$$

$$i = 1, 2, \ldots, n,$$

where d stands for the length of a range bin, i is a range bin number, and n is the total number of range bins.

A radar reflectivity factor Z and an attenuation coefficient k are empirically related to a rain rate R with the following power-law forms:

$$Z = B\,R^{\beta}$$
$$k = A\,R^{\alpha} \qquad (3)$$

where B, β, A, and α are parameters depending on radar frequency, raindrop size distribution, and others. Substituting (3) into (2) gives the following equation:

$$\log P(i+1)-\log P(i)+2\{\log r(i+1)-\log r(i)\}$$
$$= \beta\{\log R(i+1)-\log R(i)\}-0.1Ad\{R(i)^{\alpha}+R(i+1)^{\alpha}\}, \qquad (4)$$
$$i=1, 2,\ldots, n.$$

Since the left-hand side of (4) can be known from measurements, we can relate rain rates with the measurement-derived quantities if we appropriately assume the parameter values of β , A, and α . However, the number of the equation (3) becomes smaller by one than the number of rain-filled range bins, i.e., n-1, due to the ratio operation. Thus, it is impossible to determine a rain rate profile at n range bins in the present situation. Here, we introduce a path-integrated rain rate as the n-th data. The path-integrated rain rate R_{int} is defined as an integrated value of rain rate along the line of sight of the radar in km*mm/h, and is given by,

$$R_{int} = d \sum_{i=1}^{n} R(i). \qquad (5)$$

The path-integrated rain rate could be estimated from sea surface echo attenuation (Fujita et al., 1985a) of from microwave brightness temperature (Fujita et al., 1985b). The number of the data ((n-1) ratios from (4) and the path-integrated rain rate from (5)) becomes the same as that of the unknown rain rates, so that we can estimate the rain rate profile consisting of n range bins.

VERIFICATION THROUGH COMPUTER SIMULATION

To verify the performance of the proposed algorithm, we perform a computer simulation experiment assuming that the radar frequency is 35 GHz, the rain depth is 3 km, and the range-bin length d is 150 m. Thus, the number of rain-filled range bin is 20. The radar received powers are calculated with the radar equation (1) from a given rain rate profile. The radar reflectivity Z and the attenuation coefficient k are calculated from the given rain rate R by a simple power-law relation or by using raindrop size distribution of Laws and Parsons (1943) or of modified Marshall and Palmer (Olsen et al., 1978), which we are referred to as PL, LP, and MMP model, respectively (Fujita et al., 1985a). In the PL model, the parameter values of the Z-R and k-R relations are given as B=432, β=1.06, A=0.219, and α=1.04. The same values are also used in the proposed algorithm for

rain rate profiling.

In Table 1, the estimated profiles are listed for the different Z-R and k-R models. The results with and without radar signal fluctuations simulated with a zero-mean Gaussian random number are shown for each model with labels a and b, respectively. The results in a represent the average values from 20 sets of radar data having independent statistical fluctuations of its standard deviation being 10 % of the calculated received powers. Since the Z-R and k-R parameters in the PL model are the same as those for the estimation algorithm, estimated rain rates for the case without fluctuation agree with the assumed ones. For the other models, however, the estimates differ from the assumptions due to the difference in the Z-R and k-R relations from those used in the estimation algorithm. Although the probability density of signal fluctuation is symmetrical with respect to the calculated received powers, the estimates seem to have a negative bias. This would be understood to be due to the nonlinear nature in the Z-R and k-R relations for received power calculation.

	MODEL					
	PL		LP		MMP	
Assumed	a	b	a	b	a	b
7	8.5±1.0	7.0	7.9±0.6	7.3	8.4±0.7	7.2
7	7.9±0.9	7.0	9.3±0.6	7.3	8.9±0.9	7.2
7	6.8±0.7	7.0	6.8±0.7	7.3	7.1±0.9	7.2
7	6.7±0.8	7.0	6.7±0.8	7.3	7.1±0.7	7.3
7	6.8±0.8	7.0	6.9±0.7	7.3	7.0±0.8	7.3
4	3.9±0.5	4.0	3.7±0.5	3.9	3.8±0.6	3.9
4	3.8±0.6	4.0	3.4±0.4	3.9	3.5±0.4	3.8
4	3.8±0.5	4.0	4.0±0.4	3.9	4.0±0.5	3.8
4	3.8±0.5	4.0	3.7±0.5	3.9	3.6±0.6	3.8
4	3.8±0.5	4.0	3.5±0.4	3.9	3.7±0.5	3.8
7	6.8±0.8	7.0	6.6±1.0	7.1	6.9±1.2	7.2
7	6.6±1.1	7.0	6.5±1.2	7.1	6.9±1.1	7.2
7	6.6±1.0	7.0	6.5±1.1	7.1	6.8±1.0	7.2
7	6.5±1.1	7.0	6.4±1.1	7.1	6.9±1.1	7.2
7	6.6±1.0	7.0	6.3±1.2	7.0	6.9±1.4	7.2
4	3.7±0.7	4.0	3.3±0.7	3.8	3.6±0.8	3.8
4	3.7±0.7	4.0	3.3±0.6	3.8	3.6±0.7	3.8
4	3.8±0.8	4.0	3.2±0.6	3.7	3.5±0.8	3.8
4	3.8±0.8	4.0	3.2±0.6	3.7	3.5±0.8	3.8
4	3.6±0.7	4.0	3.2±0.7	3.7	4.1±1.0	3.7

Table 1. Estimated profiles for different rain models. a: Average rain rates followed by standard deviations from 20 data sets with statistical fluctuations. b: Rain rates from data without fluctuations. The unit is mm/h. The values are arranged from near to far range.

In the above simulations, correct values of the path-integrated rain rate are used to make clear the influence of the rain model. In actual cases, however, data usually include errors. To evaluate the influence of an error in the estimate of the path-integrated rain rate, additional

simulations are made for the case of the PL rain model.

Figure 1 shows the estimated and assumed profiles with and without the error in the path-integrated rain rate. As can be seen in the figure,

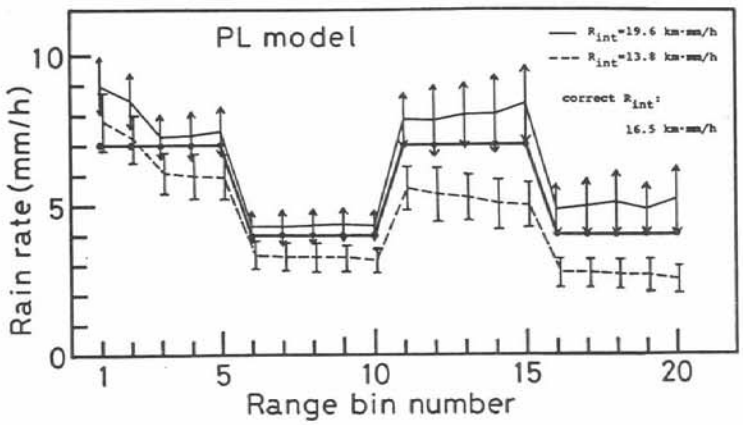

Figure 1. Estimated rain rate profiles from simulated data using the PL rain model with errors in the path-integrated rain rate.

there exists a positive or negative bias in the resulted profile depending on the sense of error, i.e., positive or negative, in the path-integrated rain rate. In addition, the absolute error in the estimated rain rate increases with increasing range from the radar. Thus, it should be said that the accurate estimation of the path-integrated rain rate would be the key of success of the present algorithm for the application to a space radar.

CONCLUSION

The author has proposed a new algorithm for rain rate profiling with an attenuating radar over the ocean. The results of computer simulation experiment have shown a promising performance. The present algorithm will be applied to aircraft data to assess the performance in a near future.

REFERENCES

Fujita, M. et al., Inference of rain rate profile and path-integrated rain rate by an airborne microwave rain scatterometer, Radio Sci., 20(3), 631-642, 1985a.

Fujita, M. et al., Quantitative measurements of path-integrated rain rate by an airborne microwave radiometer over ocean, J. Atmos. Oceanic Tech., 2(3), 285-292, 1985b.

Laws, J.O. and D.A. Parsons, The relation of raindrop size to intensity, EOS Trans. AGU, 24, 452-460, 1943.

Marzoug, M. et al., Design of a spaceborne radar for tropical rain mapping at the climatological scale, Proc. IGARSS '88 Symp., 247-248, Edinburgh, Scotland, 13-16 Sept., 1988.

Olsen, R.L. et al., The aR^b relation in the calculation of rain attenuation, IEEE Trans. AP-26(2), 318-332, 1978.

Simpson, J. et al., A proposed tropical rainfall measuring mission (TRMM) satellite, Bul. Am. Meteor. Soc., 69(3), 278-295, 1988.